Combining x-ray and photoacoustics for *in vivo* tumor imaging with gold nanorods

Guojia Huang, Sihua Yang, Yi Yuan, and Da Xing[a)]
MOE Key Laboratory of Laser Life Science & Institute of Laser Life Science, College of Biophotonics, South China Normal University, Guangzhou 510631, China

(Received 15 June 2011; accepted 29 August 2011; published online 21 September 2011)

We have demonstrated a new hybrid cancer imaging method combining x-ray and photoacoustic imaging with multifunctional gold nanorods as contrast agents. The two imaging modalities provide complementary contrast mechanisms. X-ray imaging exploits the high attenuation coefficient of gold nanorods, while photoacoustic imaging takes advantage of the strong optical absorption of the nanorods. The fused image has presented both location and vasculature of the tumor. Our experimental results demonstrate that this combined modality has the capability to provide anatomical and functional information of tumor for accurate medical diagnosis and imaging-guided therapy. © *2011 American Institute of Physics*. [doi:10.1063/1.3643033]

As one of the oldest and most widely used imaging tool, x-ray has been chosen to diagnose various diseases.[1] Specifically, it can present rich morphological information of such as the size, the shape, and the location of the tumor.[2] However, for advanced, accurate cancer diagnosis, functional information, such as vascular structure, is also needed. Photoacoustic (PA) imaging, an emerging, noninvasive imaging tool, has been used to exploit physiological parameters, such as hemoglobin concentration and oxygen saturation.[3–5] Compared to other optical technologies, PA imaging has a 100% relative sensitivity to optical absorption.[6] Different tissues with various optical absorption coefficients produce distinguishable PA signals.[7] Consequently, PA is especially appropriate for imaging of optical absorbing microstructures. As a result, blood vessels and melanoma can be distinguished by PA imaging for the fingerprint characteristics using absorption spectra.[8]

Recently, multimodal imaging which can provide complementary anatomical and functional information on biological tissues has drawn much attention in biomedical research.[9–11] X-ray computed tomography has been widely employed for cancer detection and spectroscopic PA imaging has been used to study blood vessels in mouse tumor models.[12] These two imaging modalities can make complementarity to each other with the same contrast agents of gold nanorods (GNRs). X-ray imaging exploits the high x-ray attenuation coefficient of GNRs, while PA imaging uses the high sensitivity of the tunable optical absorption of GNRs in the near-infrared (NIR) region.[13] X-ray is capable of imaging deep lesions, while PA imaging provides high spatial resolution.[14] A potential application of the combined x-ray and PA imaging is detection of breast tumor with multiparameter.[15,16]

We developed a hybrid imaging modality combining x-ray and PA imaging using pegylated GNRs (PEG-GNRs) as dual-modal contrast agents. In this letter, we report the results of using this hybrid modality for *in vivo* tumor imaging. By overlaying the site-specific functional image from PA on the background structural image from x-ray, a more comprehensive view of the tumor tissue was obtained.

An x-ray system (PiXarray 100 digital specimen radiography system, Bioptics, Inc, America) was used. The system incorporates a CCD camera with a phosphor as the x-ray detector that is irradiated with a low-power x-ray source. An optical parametric oscillator (OPO) (Vibrant 532 I, Opotek, Carlsbad, Calif) was used for PA imaging, operated at 707 nm with a pulse duration of 10 ns and a pulse repetition rate of 10 Hz. The laser beam was expanded and homogenized to illuminate the tumor with an energy density of $\sim$10 mJ/cm^2. A needle polyvinylidene fluoride hydrophone (Precision Acoustics Ltd, Dorchester, UK) with a diameter of 1 mm and a sensitivity of 850 nV/Pa was used to receive PA signals. The hydrophone, driven by a computer controlled stepper motor to scan around the mouse tumor, completed a full view of a 2π circular scan with 200 steps. The received PA signals were amplified and recorded by a digital oscilloscope (TDS3032, Tektronix, USA). A modified filtered back projection algorithm was used to reconstruct the PA images. The mouse was allowed to protrude into the water tank and insulated from the water by a piece of clear polyethylene membrane. The details of the PA system were described previously.[17]

PEG-GNRs were synthesized using a modified nonseeding synthesis protocol.[18] Then, methoxy-polyethyene glycol-thiol (MW = 5000) was added to covalently modify the surface of the GNRs. An ultraviolet-visible spectrometer (Lambda 35, Perkin-Elmer, UK) was used. The blood was obtained from a mouse, injected with heparin sodium to prevent coagulation. We mixed the PEG-GNRs and the blood with a concentration of 1.5 mg/ml. Fig. 1(a) presents normalized absorption spectra of the blood, PEG-GNRs, and blood plus PEG-GNRs. The blood spectra showed that there were two absorption peaks at 540 nm and 576 nm, respectively. The resonance absorption peak of the PEG-GNRs was at 707 nm, at which blood has a relatively weak absorption, while the blood plus PEG-GNRs maintained the 707 nm absorption peak. The inset shows a transmission electronic microscopy (TEM) image of the PEG-GNRs with an aspect ratio of 2:1.

[a)]Author to whom correspondence should be addressed. Electronic mail: xingda@scnu.edu.cn, Tel: +86-20-85210089, FAX: +86-20-85216052.

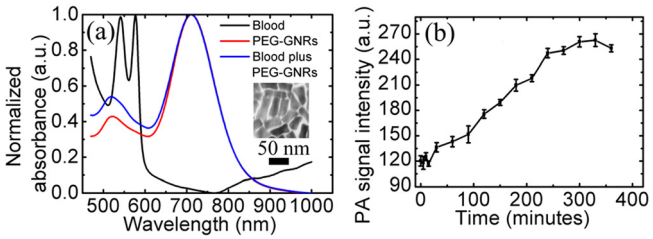

FIG. 1. (Color online) (a) Normalized absorption spectra of PEG-GNRs, blood, and blood plus PEG-GNRs. Inset: a typical TEM image of the PEG-GNRs. (b) PA signal intensity of the tumor region after PEG-GNRs injection *in vivo*. Results are a summary of three independent experiments.

Fig. 1(b) shows an increase of PA signaling in the tumor region after intravenous administration of PEG-GNRs. Thus, PA provides a unique noninvasive monitoring tool to determine the presence of light absorbing PEG-GNRs in biological systems.

In order to examine the capability of x-ray imaging to detect tumor with PEG-GNRs as contrast agents, PEG-GNRs of 200 μl (50 mg/ml) was intravenously injected via the tail vein. Figs. 2(a)–2(d) are x-ray images taken before injection, 5, 90, and 300 min post injection, respectively. In the circled region, there is a gradual enhancement of x-ray attenuation, as shown in Figs. 2(b)–2(d), compared with that in Fig. 2(a), indicating a localized tumor. To further confirm the finding, we selected a region of normal tissue (black arrows) for quantitative comparison. Fig. 2(e) shows the *in vivo* time-course of average x-ray signal intensity ratio between tumor region and normal tissue region (T/N ratio) after PEG-GNRs injection. The T/N ratio increased consistently and reached its maximum level at 300 min. The increase of T/N ratio is due to the accumulation of PEG-GNRs in the tumor region caused by enhanced permeability and retention (EPR) effect[19] and their long circulation time in the bloodstream.[20] These results suggest that with PEG-GNRs as contrast agents, x-ray is a useful tool for detecting tumor.

Furthermore, PEG-GNRs were applied to obtain noninvasive PA angiography in the tumor-bearing mouse. A 200 μl of PEG-GNRs (15 mg/ml) was injected to the mouse intravenously. Compared with the reference image in Fig. 3(a), the images in Figs. 3(b) and 3(c), obtained 5 and 90 min post-injection, respectively, revealed the tumor vasculature,

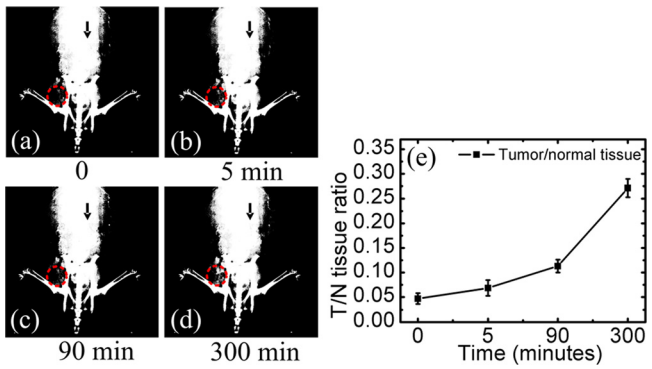

FIG. 2. (Color online) X-ray images of a mouse before injection (a), 5 min (b), 90 min (c), and 300 min (d) after injection of PEG-GNRs. (e) Time-dependent average x-ray signal intensity ratio between tumor region and normal tissue region (T/N ratio).

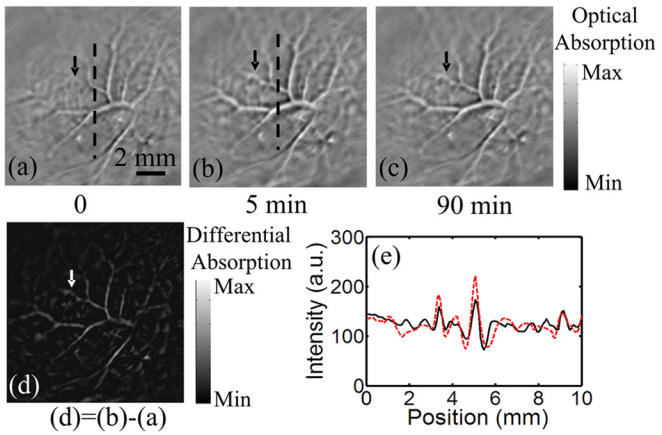

FIG. 3. (Color online) Noninvasive PA imaging of a tumor *in vivo* employing PEG-GNRs. PA image acquired before injection (a), 5 min (b), and 90 (c) min after injection of PEG-GNRs. (d) Differential image obtained by subtracting the preinjection image (Fig. 3(a)) from the post-injection image (Fig. 3(b)). (e) Reconstruction profile of image (a) (black line) and image (b) (red dash line) at the position indicated by dashed lines.

especially small blood vessels, with much clarity. This enhanced clarity was attributed to the strong PA signals generated by PEG-GNRs. The differential image in Fig. 3(d), obtained by subtracting Fig. 3(a) from Fig. 3(b), depicts the distribution of differential optical absorption in the tumor region due to injected contrast agents. Detailed tumor vascular structures, as marked by the arrows in the Figs. 3(a)–3(d), were clearly distinguished. In order to confirm the consistency of images at different times and the quantitative enhancement of PEG-GNRs, intensity profiles extracted from the images in Figs. 3(a) and 3(b), along the two lines at the same position (vertical dashed lines), were plotted in Fig. 3(e). The background and the corresponding vessels matched well. Furthermore, the signal-to-noise ratio of the two blood vessels (signal peaks in Fig. 3(e)) showed an approximate 1.5-fold enhancement, which manifests the advantages of the absorption-based PA method in imaging vascular morphology.

Coregistered x-ray image and PA image was shown in Fig. 4. The fused image clearly depicts the location and blood vessels of the tumor. Because vasculature regulates the metabolic and hemodynamic states of biological tissues, visualizing blood vessels enables tracking cancer metastasis and monitoring tumor angiogenesis. Our experimental results show that the combination of x-ray and PA imaging

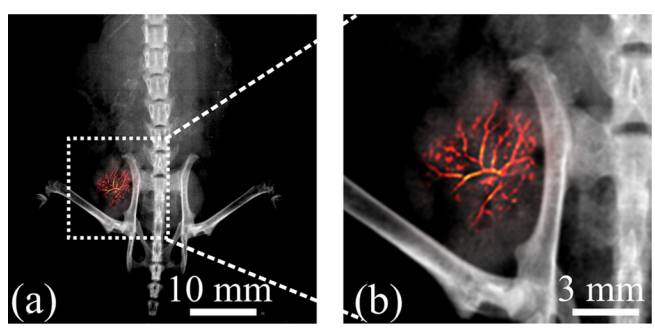

FIG. 4. (Color online) Combined x-ray and PA images of a mouse tumor *in vivo*. (a) Overlay of x-ray image and PA image. (b) Enlargement of corresponding image area highlighted by a square in panel (a).

can provide more comprehensive details of tumor such as position, size, and vascular network.

The PEG-GNRs have simplex structure, but possess multiplex function. Using the high x-ray attenuation coefficient of PEG-GNRs and their EPR effect in tumor, x-ray can distinguish the lesion and normal tissues in soft tissues. Since longer absorption peak of PEG-GNRs can be fine-tuned as a function of aspect ratio in NIR range,[21] PA can avoid intrinsic optical absorption in tissues. By modifying the surface of PEG-GNRs with target specific molecules, this hybrid modality can be used for molecular imaging of primary and metastatic tumor. For our experiments, since these two imaging methods were operated separately, there is some uncertainty to the position and orientation of the mouse. In the future, our work will focus on the establishment of an integrated x-ray-PA system.

In summary, we have developed a new multimodal imaging modality by combining x-ray and PA imaging. This hybrid imaging modality provides structural and functional properties of mouse tumor with complementary contrast mechanisms (x-ray's attenuation and optical absorption) simultaneously. Although the full potential of this modality has yet to be explored, its multimodal nature has been clearly demonstrated by *in vivo* imaging tumor in small animals.

We are grateful to Wei R. Chen for his assistance in the language. This research is supported by the National Basic Research Program of China (2011CB910402; 2010CB732602), the Program for Changjiang Scholars and Innovative Research Team in University (IRT0829), and the National Natural Science Foundation of China (30870676).

[1]P. C. Freeny, W. M. Marks, J. A. Ryan, and L. W. Traverso, Radiology **166**, 125 (1988).
[2]W. R. Chen, H. Liu, W. Yue, J. P. Wang, and R. E. Nordquist, Opt. Eng. **40**(7), 1249 (2001).
[3]G. Zh. Yin, D. Xing, and S. H. Yang, J. Appl. Phys. **106**, 013109 (2009).
[4]H. F. Zhang, K. Maslov, M. Sivaramakrishnan, G. Stoica, and L. V. Wang, Appl. Phys. Lett. **90**, 053901 (2007).
[5]J. Laufer, C. Elwell, D. Delpy, and P. Beard, Phys. Med. Biol. **50**, 4409 (2005).
[6]L. Li, K. Maslov, G. Ku, and L. V. Wang, Opt. Express **17**, 16450 (2009).
[7]K. Kim, S. W. Huang, S. Ashkenazi, M. O'Donnell, A. Agarwal, N. A. Kotov, M. F. Denny, and M. J. Kaplan, Appl. Phys. Lett. **90**, 223901 (2007).
[8]C. H. Kim, E. C. Cho, J. Y. Chen, K. H. Song, L. Au, C. Favazza, Q. Zhang, C. M. Cobley, F. Gao, Y. N. Xia, and L. H. Wang, ACS Nano **4**(8), 4559 (2010).
[9]C. Vinegoni, T. Ralston, W. Tan, W. Luo, D. L. Marks, and S. A. Boppart, Appl. Phys. Lett. **88**, 053901 (2006).
[10]L. S. Bouchard, M. S. Anwar, G. L. Liu, B. Hann, Z. H. Xie, J. W. Gray, X. D. Wang, A. Pines, and F. F. Chen, Proc. Natl. Acad. Sci. U.S.A. **106**(11), 4085 (2009).
[11]S. Jiao, Z. Xie, H. F. Zhang, and C. A. Puliafito, Opt. Lett. **34**, 2961 (2009).
[12]Y. Q. Lao, D. Xing, S. H. Yang, and L. Zh. Xiang, Phys. Med. Biol. **53**, 4203 (2008).
[13]W. Ch. Law, K. T. Yong, A. Baev, R. Hu, and P. N. Prasad, Opt. Express **17**, 19041 (2009).
[14]D. Razansky, M. Distel, C. Vinegoni, R. Ma, N. Perrimon, R. W. Koster, and V. Ntziachristos, Nat. Photonics **3**, 412 (2009).
[15]S. Manohar, S. E. Vaartjes, J. C. G. van Hespen, J. M. Klaase, F. M. van den Engh, W. Steenbergen, and T. G. van Leeuwen, Opt. Express **15**, 12277 (2007).
[16]F. Ye, S. H. Yang, and D. Xing, Appl. Phys. Lett. **97**, 213702 (2010).
[17]S. H. Yang, D. Xing, Y. Q. Lao, D. W. Yang, L. M. Zeng, L. Zh. Xiang, and W. Chen, Appl. Phys. Lett. **90**, 243902 (2007).
[18]N. R. Jana, Small **1**, 875 (2005).
[19]H. Maeda, Adv. Drug Delivery Rev. **46**,169 (2001).
[20]S. Kommareddy and M. Amiji, J. Pharm. Sci. **96**, 397 (2007).
[21]S. Link, M. B. Mohamed, and M. A. El-Sayed, J. Phys. Chem. B **103**, 3073 (1999).